Vilnius University
Faculty of Physics

Rana Nabeel Ahmad

PEO-based triboelectric nanogenerators

Master's final thesis
Electronics and Telecommunication Technologies

Student	Rana Nabeel Ahmad
Approved	2026-05-22
Academic supervisor	Doc. Martynas Kinka
Director/ representative of the Institute / Center	prof. Robertas Grigalaitis

Vilnius 2026

Table of Contents

INTRODUCTION

Increasing demand for sustainable energy has driven attention of researchers to alternative energy-harvesting technologies and triboelectric nanogenerators (TENGs) have emerged as promising approach for converting mechanical energy into electrical energy [1]. TENGs work on the principles of triboelectrification and electrostatic induction, which make the harvesting of energy from the ambient sources like vibrations, human motion and wind possible [2]. They have a high-power density and are also cost effective and suitable for flexible and wearable applications [3].

Polyethylene oxide was noticed as a positive triboelectric material because of its incredible biocompatibility, processing convenience and great triboelectric properties [4]. PEO based TENGs are superior in performance when used with electron accepting materials like PDMS and metal electrode. Some preliminary research also investigated the effects of addition of fillers such as aluminum, copper, barium titanium oxide, carbon nanotube, etc. These materials showed that there is a visible improvement in the performance of TENGs based on PEO [5], and among them, silicon carbide particles showed excellent performances based on their high polarization effect and Dielectric Constant, which led to an improvement in charge retention and the ability of the material to transfer charges [6]. The relationship between SiC concentration and TENGs performance, however, may need to be investigated, specifically their relationship with the various loading levels for the TENGs performance. This study proposes how changing concentration of SiC may affect the performance of PEO based TENGs.

The aim of the work is to investigate the potential of polyethylene oxide (PEO) - based composites for mechanical energy harvesting in triboelectric nanogenerator (TENG) devices. During the work pure PEO and PEO based composite films will be casted and their triboelectric properties will be investigated in several TENG configurations towards increasing the efficiency of mechanical energy conversion into electrical power.

Objectives:

1. To prepare and fabricate PEO-based composites films with different materials and concentrations for TENG application.
    - To prepare PEO film samples on Aluminum and Copper.
    - To prepare PEO film samples incorporated with BaTiO3, CNT, SiC and SiC with varied concentration placed over copper using spin coating.
2. To test triboelectric performance of prepared samples on TENG device.

- Measurement of short circuit current with Al, Cu, PDMS/Al and PDMS/Cu in vertical contact separation.
- Measurement of surface charge density (nC/cm^2).
- Measurement of load voltage and load current of all prepared samples

3. To evaluate optimal power through TENG device.
    - For optimal power, calculate power density for prepared sample and eventually how PEO based triboelectric nanogenerator influenced with addition of impurities with specified concentration at room temperature.

LITERATURE REVIEW

2.1 Introduction to TENGs

The use of green and sustainable energy has received a lot of attention due to the growing threats of environmental pollution and the need for energy. Many efforts have been made to harvest various forms of energy from various natural sources, including solar, wind, and hydro [7], and convert them into useful electrical energy. The most dominant of them is mechanical energy, which can originate from gravity, water, and wind. The capacity of triboelectric nanogenerators to capture mechanical energy and convert it into sustainable electrical energy has attracted a lot of interest. Through a variety of techniques, including electrostatic induction and the coupling effect of contact electrification, they can transform mechanical energy into electrical energy [8].

Since its initial display, TENG has been extensively investigated and admired. TENG offers several benefits, including flexible structural design, low cost, and high-power generation. TENG can function in electrode contact, single electrode contact, and sliding modes [9]. In contact mode, it consists of two insulators with electric polarities that are far apart in a triboelectric series so that, upon contact and subsequent separation, one material acts as a donor and the other as an acceptor. We refer to the donor material as positive triboelectric and the acceptor material as negative triboelectric because our goal is to maximize output power, which can be achieved through increased surface charge density. The only effective way to boost TENG's efficiency is to choose the best material with a high electron affinity difference and costly equipment. As a result, the TENG cost increases significantly, making the use of these methods impractical.

2.2. Triboelectric Effect and Triboelectric Series

TENG uses electrostatic induction and triboelectric phenomenon to transform mechanical energy into electrical energy. In the inner circuit, the charge transfer between two thin organic/inorganic films with opposing tribopolarity generates potential, and in the outer circuit, the electrons transfer between two electrodes attached to the back of the films so that the potential in the outer circuit is balanced in accordance with the potential generated in the inner circuit [10]. The built-in potential of TENG is dependent upon the use of electrodes. The relative position of the tribomaterial in the triboelectric series may change depending on the choice of the electrode due to the use of potential for enhancing the electrical performance by increasing electron charge density. Because of their availability and high conduction properties, Al and Cu are the most often used electrodes. The triboelectric series is also crucial to understanding how charge transfer works in the case of triboelectric nano generators, which rate materials according to how likely they are to gain or lose

electrons when they come into contact with one another but only if they are in their place. The combinations of these materials have a great effect on the output performance due to the tendency of materials close to the positive side to lose electrons and materials close to the negative side to gain more electrons. Materials such as polyethylene, which are on the negative side of the trend, have high electron affinity, as shown in figure 1. With the materials located nearer to the positive side, such as Al and Cu, the pair can act as an effective triboelectric pair and the polarity difference between the materials can lead to better results and output characteristics.

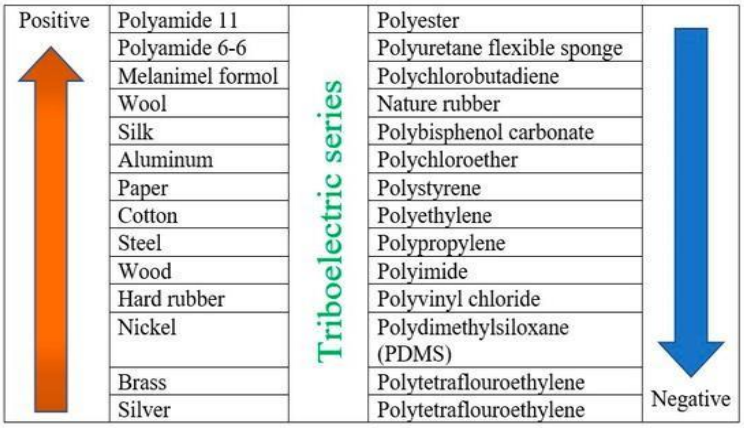

Figure 1: Triboelectric series with the positive and negative characteristics.[7].

2.3. Working principle of TENGs:

A TENG operates on the most basic principles of electrostatic and triboelectric effects [11]. Triboelectrification, also known as contact electrification, is a phenomenon that occurs when two distinct substances come into touch with one another. It is the basis for how TENG operates. When two different materials come into contact with one another as a result of external mechanical energy, electrostatic charges are induced in them. When the external mechanical energy separates them again, an electrical potential is created between these electrostatic charges, causing the charges on these materials to move from one side to the other. This process of charge movement is irreversible. Hence the excess charges accumulate on one side and deficit charges on other side and alternating current can flow according to charge polarity [12]. The schematic illustration of working of TENG is shown in figure 2.

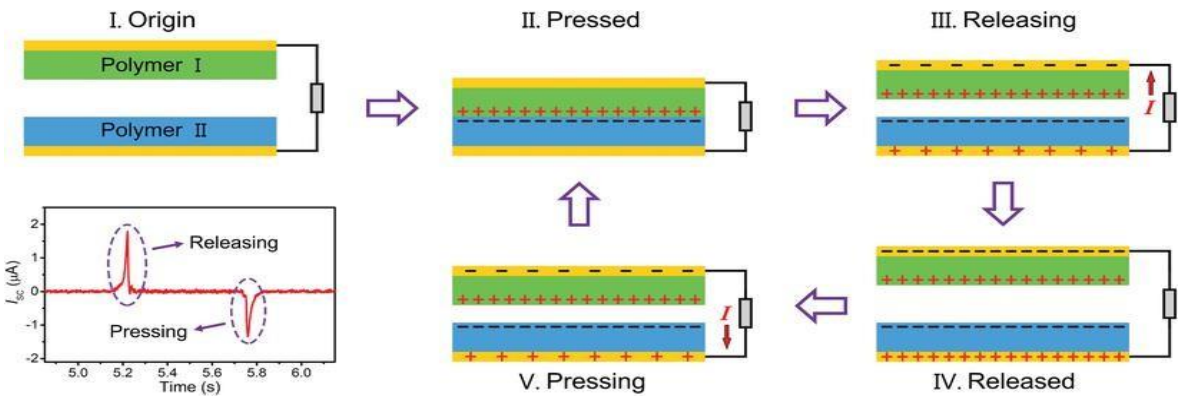

Figure 2: Working principle of the TENG in contact-separation mode [12].

As seen in figure. 3, TENG operates in four main modes: vertical contact separation, freestanding triboelectric layer, single electrode, and lateral sliding. Both materials move relative to one another perpendicular to the interface during vertical contact separation. This creates a potential difference, which causes a current flow to counteract the impact. A potential difference is created when lateral sliding movement is parallel to the interface. In single electrode mode, earth acts as the reference electrode and mechanical energy is captured without the need for a conduction line. Two symmetric electrode pairs are employed in the FT mode. The unequal charge distribution generates an electrical output due to separation of freely moving charges [13].

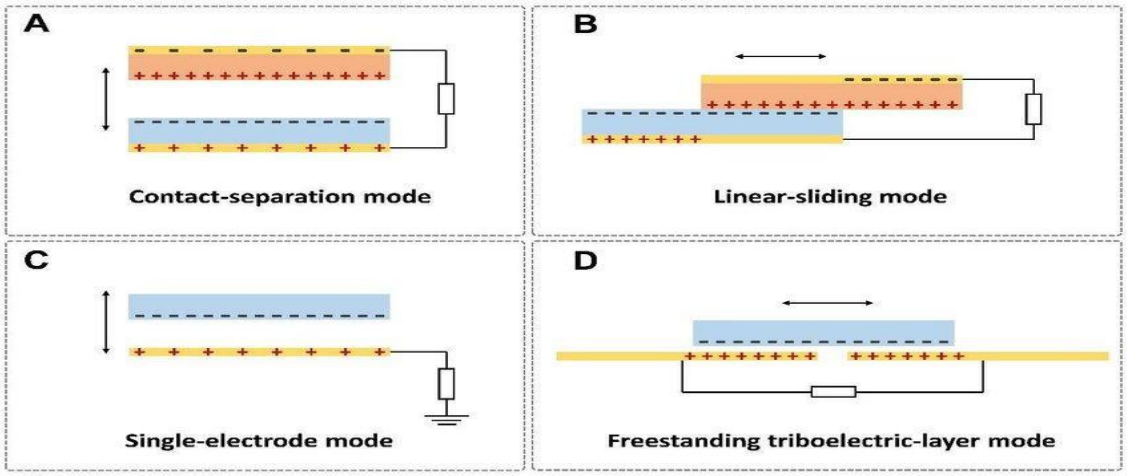

Figure 3: The four working modes of TENG.[14].

figure 4 illustrates the four primary levels of TENG: the charge-generating layer, the charge-trapping layer, the charge-collecting layer, and the charge-storage layer. When two charge-generating layers first come into touch with one another by mechanical force, electron transfer occurs, and one layer becomes positively

charged while the other becomes negatively charged. The charge that was transferred between them is then sent to the charge storage layer after being shunted via the charge trapping and collecting layer during the subsequent cycle [15]. The TENG layers are depicted in the Figure [4] below.

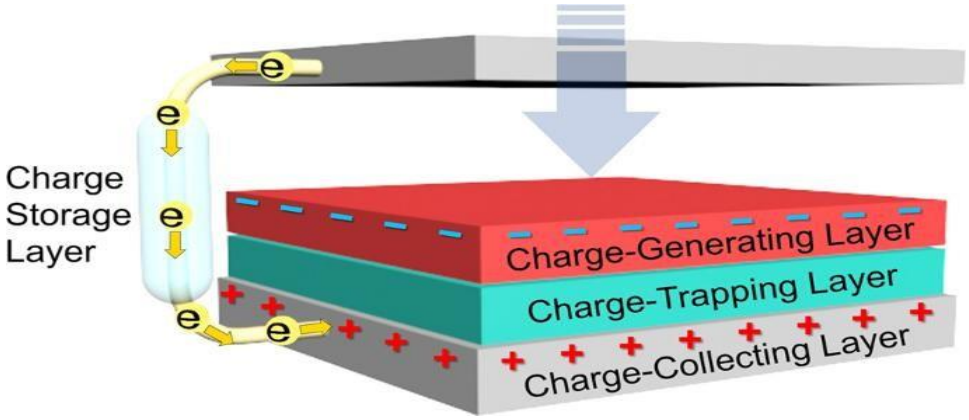

Figure 4: Four different layers of TENG [16].

Ion transfer, electron transfer, and material transfer are the three primary triboelectrification processes. Triboelectric charging occurs because of imbalanced charges brought on by ion transfer. Large particles of material are exchanged when surfaces come into touch with one another; this might happen as a result of a chemical reaction or surface roughness [17].

2.4. Theoretical Model of Contact-Separation TENG

The interaction between voltage, charge transfer, and separation distance determines how TENG functions in contact separation. The V-Q-x relationship provides the voltage for a parallel plate capacitor model with two dielectric layers in contact. When the surfaces split, the voltage increases for open circuit voltage. Surface charge density, separation distance x, and the material's dielectric characteristics all affect the open circuit voltage. A short-circuit transferred charge Q_{SC} is produced when charges flow via an external circuit under a short circuit state.

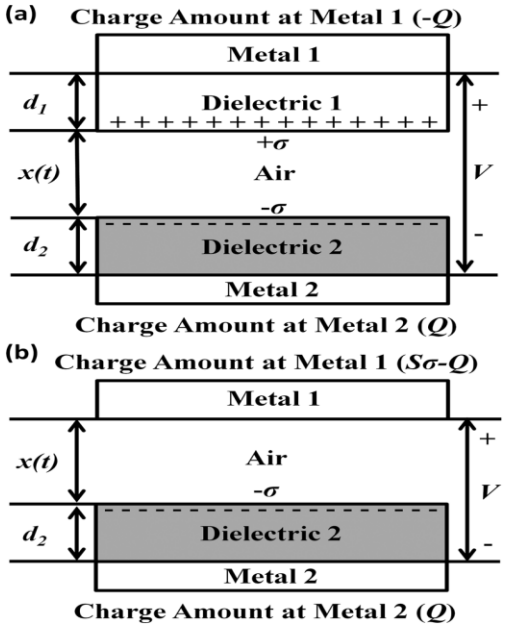

Figure 5: Theoretical model of TENG [18].

There are two cases shown in figure 5 above. 1st case is dielectric to dielectric in such case there are two dielectric layers of thickness d1 and d2 and having relative dielectric constant of $\boldsymbol{\varepsilon_{r1}}$ and $\boldsymbol{\varepsilon_{r2}}$ they are used as triboelectric layer and on the outside layer two metals are used, and their distance is varied accordingly. Between these dielectrics, there is an air gap and inside these dielectric and air gaps electric field only has a component pointing in perpendicular direction to surface. And their electric field strengths according to gauss theorem are given by;

$$\boldsymbol{E_1} = \frac{-\boldsymbol{Q}}{\boldsymbol{S\varepsilon_0\varepsilon_{r1}}} \tag{1}$$

$$\boldsymbol{Eair} = -\frac{\frac{\boldsymbol{Q}}{\boldsymbol{S}}+\boldsymbol{\sigma(t)}}{\varepsilon_0} \tag{2}$$

$$\boldsymbol{E_2} = -\frac{\boldsymbol{Q}}{\boldsymbol{S\varepsilon_0\varepsilon_{r1}}} \tag{3}$$

$$\boldsymbol{V} = \boldsymbol{E_1 d_1} + \boldsymbol{E_{air}} + \boldsymbol{E_2} \tag{4}$$

$$\boldsymbol{V} = -\frac{\boldsymbol{Q}}{\boldsymbol{S\varepsilon_0}}\left(\frac{\boldsymbol{d_1}}{\boldsymbol{\varepsilon_{r1}}} + \frac{\boldsymbol{d_2}}{\boldsymbol{\varepsilon_{r2}}} + \boldsymbol{x(t)}\right) + \frac{\boldsymbol{\sigma x(t)}}{\boldsymbol{\varepsilon_0}} \tag{5}$$

In above equations Q represents the charges generated, σ is the surface charge density and S represents area size of the metals. For second case as shown in fig 5b, metal 1 acts as an electrode since there is only one dielectric which will act as acceptor. Therefore, the equation for voltage for this case becomes;

$$\boldsymbol{V} = \boldsymbol{Ed_2} + \boldsymbol{E_{air}} \tag{6}$$

$$V = -\frac{Q}{S\varepsilon_0}\left(\frac{d_2}{\varepsilon_{r2}} + x(t)\right) + \frac{\sigma x(t)}{\varepsilon_0} \qquad (7)$$

If, in equation of voltage we replace $\frac{d_1}{\varepsilon_{r1}} + \frac{d_2}{\varepsilon_{r2}}$ with d_0 we will get

$$V = -\frac{Q}{S\varepsilon_0}\left(d_0 + x(t)\right) + \frac{\sigma x(t)}{\varepsilon_0} \qquad (8)$$

And in short circuit condition V=0 hence after solving above equation, we get;

$$Q_{sc} = \frac{S\sigma x(t)}{d_0 + x(t)} \qquad (9)$$

Transferred charge is maximum when surfaces are fully separated.

Short circuit current is time derivative of charge being transferred

$$I_{sc} = \frac{dQ_{sc}}{dt} \qquad (10)$$

Replacing the value of Q_{sc}, and after solving this equation we get

$$I_{sc} = \frac{S\sigma d_0 v(t)}{\left(d_0 + x(t)\right)^2} \qquad (11)$$

The maximum short circuit current is observed for fastest separation or approach phase.

At open circuit condition, when Q is 0 because of no charge transfer in open circuit conditions. Therefore, Voc is given by;

$$V_{oc} = \frac{\sigma x(t)}{\varepsilon_0} \qquad (12)$$

Voc is directly proportional to separation distance and increases linearly with separation distance and is inversely proportional to effective dielectric thickness of each layer and materials with high relative permittivity ε_r reduce the voltage while thinner layer increases the voltage.

2.5. Power Output and Enhancement Strategies

The electrode materials in the triboelectric nanogenerator play a very important role in transferring the triboelectric charges to an external circuit. Aluminum (AL) and copper (Cu) are both good conductors of electricity, rigid and have good bonding ability with the dielectric material. When Al is used with Cu, however, due to its low output voltage, friction is reduced in order to minimize abrasion [19].

Output voltage for the copper foil was 78.8 V and the current was measured as 12 µA, hence the selection of the appropriate material of the electrodes plays a vital role in achieving the best results [20]. In some studies, the electrical performance of TENG was investigated by using aluminum and copper electrodes and some of the materials were evaluated according to the performance of TENG used in the single electrode mode. Another study [21] showed that, utilizing a few layers of graphene-based electrode in TENG, the power density was 26 times higher. The negative electron affinity materials such as (PDMS), (PVDF) and polytetrafluoroethylene (PTFE) are best ones for enhancing TENG performance. However, not much has been done on positive triboelectric materials.

It was believed that the PA6 was the best material among tribo-positive materials to use for the fabrication of TENG because of its high positive polarity. But recently PEO emerged as the more positive and less costly alternative to PA6. Polyethylene oxide, also known as PEO, is a synthetic, inexpensive, soluble in water and biodegradable commodity polymer. The triboelectric properties of PEO/PDMS are much more positive than those of polyamide-6 (PA6) PEO/PDMS [6]. The output efficiency of the TENG is closely related to polymer-electrode contact, which has an important influence on it. It is therefore very important to have an optimal interaction, both for maximum output power and maximum efficiency.

When mixed with metal electrodes such as Al and Cu PEO's structural support and electrical conductivity will be enhanced. The analysis revealed that Al has benefits in terms of cost and weight, and in terms of generating and transferring electricity, which enhances performance [22]. If PEO with copper is used, blistering problems can be avoided, and good anti-corrosion and fouling resistance will be given [23].

2.6. Polymer Composites for Performance Enhancement

Recent research has shown that incorporation of different high dielectric fillers can be used as an effective means of enhancing output performance by increasing surface charge density. Being a high dielectric constant material, BaTiO3 has gained significant interest amongst the different fillers due to its ability to cause interfacial polarization and increase the surface charge density when distributed in elastomeric matrices such as PDMS [24]. In another example, the use of semiconducting fillers in polymer composite such as silicon carbide (SiC), to enhance the electrical insulation and charge trapping property, has resulted in a high triboelectric output and good operational stability [6]. In addition, the high specific surface area and high electrical conductivity enable easy charge transit in the polymer layers and facilitate the modification of their surface shape to enhance the electrical performance of the layers, which is why carbon nanotubes (CNTs) are often incorporated into the polymer triboelectric layers [25]. These studies show that the electrical and interface properties of polymer composites can be modified effectively by adding dielectric, semiconducting and conductive fillers as compared to the conventional Al/Al, Al/Cu and PDMS/Cu TENG configurations.

This can be used as a good starting point to examine the properties of the modified layers (BaTiO3, SiC and CNT's) in the PEO.

A paradigm change in material design techniques was brought about by the creation of composite-based TENGs. The researchers succeeded in enhancing the surface charge density and the dielectric properties by introducing functional filler [26]. Ceramic nanoparticles, such SiC and BaTiO3, have drawn a lot of interest among other materials because of their elevated dielectric constants and polarization capacities. Further, the BaTiO3 SiC-filled composites also had higher output power and charge retention than the other composites.

SiC with excellent electrical properties, high thermal stability and high mechanical strength has appeared to be a very attractive filler for polymer matrices like PEO. According to the proposed mechanism, SiC nanoparticles will be integrated with PEO based TENG's to enhance the performance, because of its higher surface area and charge transfer ability. SiC in optimum concentration can substantially improve voltage and power density. The mechanism through which SiC enhances performance of PEO based TENG's can be attributed to several factors, one of which is that incorporation of SiC nanoparticles influences microstructure and phase of pro matrix that leads to improved charge generation and transfer [6]. In particular, the electrical performance is improved by the increase in the interfacial area for charge separation and transfer.

Future research work can be helpful in finding the optimum concentration range of SiC to further improve the performance of PEO based TENG's and maximize energy transfer from TENG's.

From the existing literature, there has been definite development progress regarding the development of TENG materials; however, the relationship between the concentration of the fillers and the performance had not been studied yet, and this is well understood. Studies in literature are also concerned with loading the material with fillers to increase the dielectric properties, but it is also possible to optimize the performance by determining optimal concentrations.

In the present study, the problem is being solved by studying the effects of varying concentrations of SiC in PEO composites. In contrast with previous works which concentrated on the selection of the best material, we show that the optimal SiC concentration can be used to enhance performance by optimizing charge transfer dynamics. This will bring into question the current paradigms and give new ideas for TENG improvement.

2.7. PEO and PDMS in TENG Applications

PEO is a flexible material. It contains c-o-c in high density that gives it a high positive polarity in the triboelectric series, PEO is a linear semicrystalline. A flexible positive triboelectric material is polyethylene oxide (PEO). The high positive polarity in the triboelectric series, resulting from the high density of c-o-c, makes it suitable to use it as a positive friction layer, and the repeating ether motifs can facilitate the transfer of charges of the surface during the contact separation process [4]. PEO has certain unique properties due to its simple and flexible structure, which is a linear semicrystalline polymer. The crystallinity and glass transition temperature of the PEO can be changed by varying the molecular weight of PEO, for example by

changing the salt concentration and adding other polymers [27]. The triboelectric property of PEO has been recently proposed to be enhanced by changing its shape and by adding chemicals. The addition of AgSiO2 to improve the output, due to its higher dielectric constant and surface roughness [28].

Technically, PEO is a rich and viable material for study of electrode pairing and dielectric response for TENG performance, while practically, it is a suitable host material for synthesis of PEO-based composites. Molecular structure of PEO is given in figure 6. Hao et al. [4] pointed out the importance of polyethylene oxide as a positive triboelectric material. This material has the following features: Excellent dielectric property, film forming property and environmental friendliness. It also directly contributes to the research of PEO films on aluminum and copper. Because of its great tribo-positivity, PEO is frequently utilized as a positive triboelectric generator in TENG arrangement.

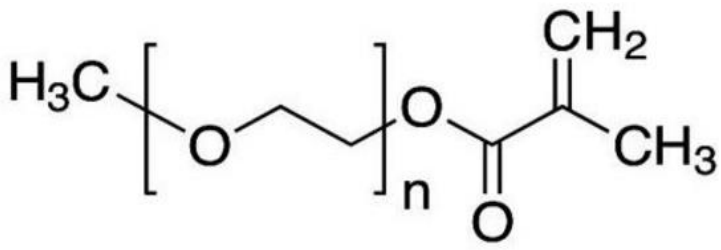

Figure 6: Molecular structure of polyethylene oxide (PEO).[29]

PEO is a polar polymer with oxygen containing functional groups that tend to lose electrons when in contact whereas PDMS with its siloxane and methyl side groups tend to gain electrons. This large separation ensures high surface charge density when in contact.

METHODOLOGY

3.1 Material Selection

For our experiment we used 600 000g/mol of PEO as a dielectric material and Al, Cu and PDMS with Al and Cu were used as electrodes. Various number of composites of BaTiO3, CNT's and SiC, and SiC whiskers in a varying quantity prepared and incorporated over PEO, and Triboelectrification is investigated. Detailed sample preparation is mentioned below;

3.2 Sample and Composite preparation

To determine the effect of the electrode material and nanocomposite fillers on the performances of TENG devices, several thin films were fabricated based on the standard fabrication methods. This base polymer solution was obtained by dissolving 0.3 g of polyethylene oxide (PEO) powder in 10 mL of distilled water and then continuously stirring the solution with a magnetic stirrer for 24 hours at room temperature to ensure complete dissolution and achieve a high viscosity for uniform film deposition. The solution obtained was then deposited onto aluminum (Al) and copper (Cu) substrates in a Polo Spin 150i spin coater at 800 rpm for 120 s. Residual solvent was removed and the integrity of the films consolidated by thermal drying of the coated substrates at 60 °C for 10 minutes.

The effect of the electrode material on the device output was tested by preparing six different top/bottom electrode configurations. Al, Cu and polydimethylsiloxane (PDMS) were used in combination as the top electrodes and the resulting combinations are as follows: Al/PEO_Al, Cu/PEO_Cu, Al/PEO_Cu, Cu/PEO_Al, Al/PEO-PDMS_Cu, and Cu/PEO-PDMS_Cu. The adopted geometry of each device was of a sandwich type, and they were all used in the vertical contact-separation mode, with the aim of providing uniform and comparable mechanical excitation in all the configurations. PEO thin film was deposited on Al and Cu to form dielectric-electrode assemblies constituting upper and lower components of device and when PDMS is added as additional dielectric it increases effective permittivity and thickness of dielectric device.

After testing these electrode configurations, we used three active filler materials which were then incorporated into the polymer matrix: multi-walled carbon nanotubes (CNTs); spherical silicon carbide (SiC), with average diameter of 80 nm and barium titanate ($BaTiO_3$). The base polymers are obtained by dissolving 0.3g of PEO in 10g distilled water, and 0.108144g of MWCNT is added to solution. For barium titanium oxide, 0.3g of PEO was added to 10g of distilled water, later added 3.15528g of 300 nm $BaTiO_3$. For Silicon carbide whiskers, 0.15g of PEO was added 5mL distilled water. 0.0828g of SiC was added to this solution. All these mixtures are continuously stirred for 24 hours with magnetic stirrer to obtain homogeneous composite solutions.

The homogenous composites solutions were placed over copper substrate. Every substrate has a surface area of 2.5 x 2.5 cm^2. Because of its impacted electrical characteristics, this substrate is perfect for Triboelectric Nanogenerator (TENG) applications.

Following the spin-coating procedure, the produced samples were heated to 110°C for three hours on a hot plate. A stable, functioning sample that is prepared for testing is produced by this last heat treatment, which guarantees that the composite film is securely bonded to the substrate. The sample preparation was done using polyethylene oxide in powdered form with molecular weight of 600,000 (nominal) and silicon carbide whiskers. The physical properties used were as follows

To achieve thin films composite solutions were deposited on substrates using a spin coater. To maintain film quality under different viscosities the spin speed was adjusted in an incremental manner for higher concentrations and maximum spin speed for about 120 seconds for a concentration of 5 vol%

Table 1: Test samples against their spin speed.

Sample (vol% SiC)	**Spin Speed (rpm)**
0.025 vol%	400
0.05 vol%	400
0.045 vol%	500
0.1 vol%	500
0.3 vol%	600
0.5 vol%	700
1.0 vol%	800
5.0 vol%	1200

TENG device was assembled according to film fabrication. The composite PEO-SiC film served as primary triboelectric layer. Copper top contact integrated with PDMS layer for that PDMS was spin coated on same Cu foil at 800 rpm for 2 minutes and thickness of PDMS was 0.0886mm. This served as counter-electrode layer.

3.3 Experimental Setup

The whole experimental setup used to assess output characteristics during the previous semester is depicted in the pictures below. The device's output performance, including output voltage, current, and other characteristics, was measured using a repeated vertical compression force of around 20 N at various frequencies ranging from 1 Hz to 1 MHz. An electric generator (LABPS3005DN) that produced a 12 V electric pulse at the necessary frequency via relay was utilized to operate a pushing plunger for periodic blows.
Using a 3D printer, a rectangular tip for direct sample contact was created and affixed to the electromagnet's movable component. An oscilloscope was used to measure the output voltage on the sample, and an adapter was attached to the oscilloscope to export the data straight into a computer for processing and real-time results monitoring. figure 7 depicts the completed circuit with plunger and loads, whereas figure 8 depicts the schematic of experimental set-up.

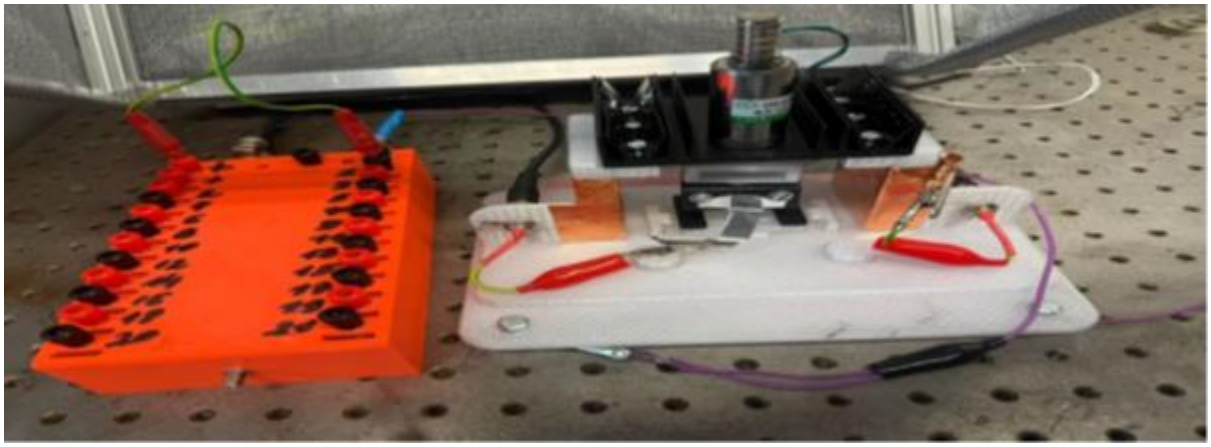

Figure 7: Contact separator circuit with loads and plunger used to determine output parameters

For this time, we used a new TENG device as shown below in figure 8. This setup is basically a test rig for vertical contact separation TENG, generated repeated mechanical contact between two triboelectric surfaces. During each downward stroke the moving sample met fixed lower sample. This periodic contact separation caused triboelectric charges to build up on the surface resulting in a potential difference. The output of device was connected with the voltmeter/ammeter for calculating V_{OC} and I_{SC} with a relay, which is further connected with digital oscilloscope. Further, this TENG is also connected with load for calculating V_L and I_L. In this TENG device, contact time and separation time are kept same which is 100 milliseconds.

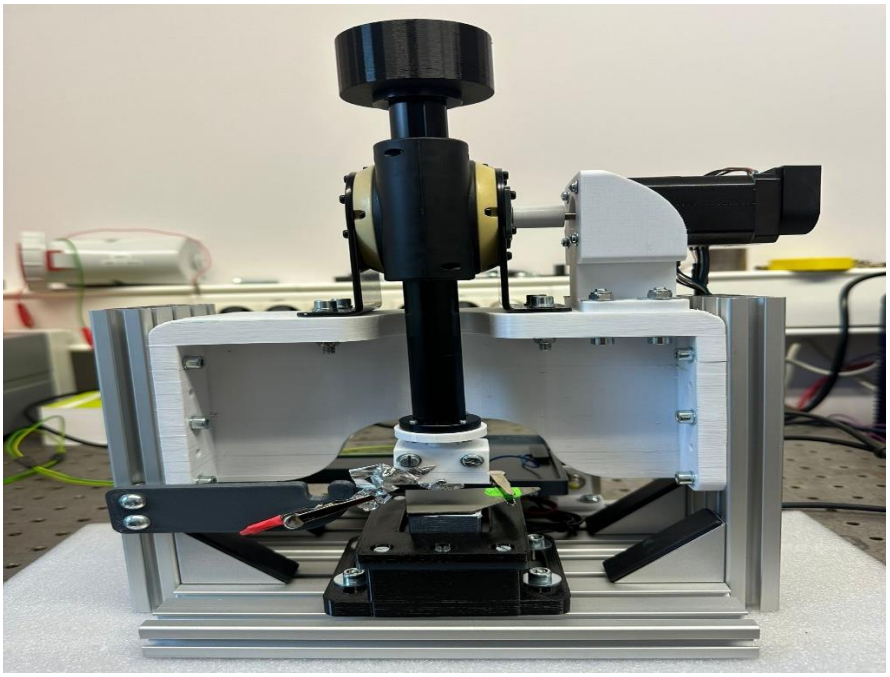

Figure 8: TENG device to determine output parameters.

RESULTS AND DISCUSSIONS

This study was conducted in three phases and the findings from each phase motivated to investigate new samples. Results and Discussions are characterized into three phases;

- Pure PEO
- PEO with SiC, $BaTiO_3$, CNT's
- PEO with different SiC concentrations

Triboelectrification is investigated by measuring open circuit voltage (V_{OC}), short circuit current (I_{SC}), surface charge density (σ) and load dependent output of devices (P_{LOAD}) from which the peak power density (Pd) was calculated. The results are presented and illustrated below in the logical order.

4.1 Pure PEO:

To study the triboelectric output of the fabricated TENG's using a PEO-based dielectric film as the active triboelectric layer and a combination of six different electrode was used, along with counter layer configurations which were designed and estimated. Our TENG device is based on same vertical contact separation mode as mentioned in figure 05, [18]. For TENG devices we have two mechanism, top electrode and bottom contact both are dielectric materials (PDMS-Al and PDMS-Cu on top and PEO-Al and PEO-Cu on bottom) as shown in figure 05 (a), and top electrode as metals (Al and Cu) and bottom contact as dielectric material (PEO-Al and PEO-Cu) as shown in figure 05 (b) [18].

The experimental Open Circuit voltage (Voc) values align with the theoretical behavior predicted by Equation (12) which states that Voc output is directly proportional to the generated surface charge density, σ. The Al/PEO-Al and Cu/PEO-Cu samples acted as per the single-dielectric model of Fig. 5(b), and so Eq. (12) was used to analyze the voltage generation mechanism. Although the work-function differences are very small for the same metals, the electrostatic charge generated at the interface was small, so the output voltage was relatively small. figure 9 shows combined graph of open circuit voltage. The Cu/PEO-Cu configuration was slightly better because of the difference in electronegativity between Cu and Al, but the Voc was still around 1.6 V for the Al/PEO-Al configuration. For metals pair configuration of Al/PEO-Cu and Cu/PEO-Al, the devices were still operated according to the figure 5(b) configuration, and the results were analyzed by the equations (7) and (12).

The surface potential difference significantly increased, increasing the triboelectric charge density, and thus the output voltage. Al/PEO-Cu configuration resulted in the production of around 6.5V, whereas the Cu/PEO-Al configuration resulted in the production of near 9-10V. This can be attributed to the higher electronegativity difference between Cu and Al which enhanced the charge transfer at the interface and thus increased the σ according to Equation (12).

$$\mathbf{V_{oc}} = \frac{\sigma x(t)}{\varepsilon} \qquad (12)$$

When PDMS was used as the counter triboelectric layer, a much better results were obtained. The devices of Cu-PEO/PDMS-Cu and Al-PEO/PDMS-Cu, which had a dual-dielectric structure as shown in figure 5(a), were analyzed by Equations (1) to (5) for the voltage generation mechanism.

$$\mathbf{E_{d1}} = -\frac{Q}{S\varepsilon_o\varepsilon_r 1} \qquad (1)$$

$$\mathbf{E_{air}} = -\frac{\frac{Q}{S}+\sigma(t)}{\varepsilon_o} \qquad (2)$$

$$\mathbf{E_{d2}} = -\frac{Q}{S\varepsilon_o\varepsilon_r 2} \qquad (3)$$

$$V = \mathbf{E_{d1}} + \mathbf{E_{air}} + \mathbf{E_{d2}} \qquad (4)$$

$$V = -\frac{Q}{S\varepsilon_o}\left(\frac{d1}{\varepsilon_r 1} + \frac{d2}{\varepsilon_r 2} + x(t)\right) + \frac{\sigma x(t)}{\varepsilon_o} \qquad (5)$$

$$V = \mathbf{E_{d2}} + \mathbf{E_{air}} \qquad (6)$$

Nearly 90 V was obtained for the PDMS/PEO-Al configuration and nearly 57 V was obtained for the PDMS/PEO-Cu configuration. The strong enhancement is due to the highly electronegative attribute of PDMS, which is more on the negative end of the triboelectric series due to its siloxane backbone and methyl side groups. On the other hand, PEO has electron donating ether linkages (C–O–C) which lead to an extremely large polarity difference between PDMS and PEO. This large polarity difference led to a high surface charge density of the triboelectric charging σ and hence to a higher Voc as expressed in Equation (12).

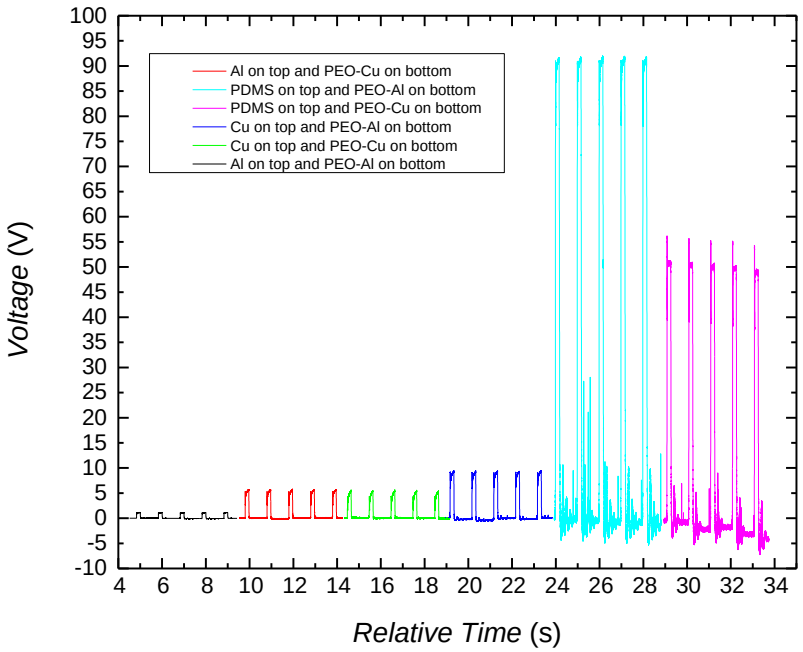

Figure 9: Open circuit voltage.

The short circuit current trends were similar to that of Equation (11)

$$\mathbf{I_{sc}} = \frac{S\sigma d_o v(t)}{(d_o + x(t))^2} \qquad (11)$$

Figure 10 shows short circuit current graphs obtained for these configurations. The devices with larger current output had the higher triboelectric charge densities, as I_{SC} is directly proportional to σ and the active separation process. Peak currents from 0.02-0.05μA were obtained from the metal-only configurations and currents as high as 0.2μA were obtained from the PDMS/PEO-Al containing structures which is the highest current obtained in this phase followed by PDMS/PEO-Cu which exhibited nearly 0.019 μA current peak .

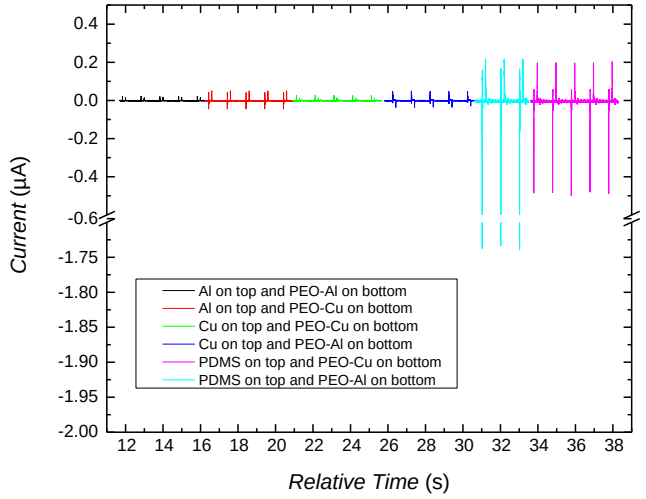

Figure 10: Short Circuit current

The electrical measurements were also measured dependence on load, which were further confirmed the capacitive nature of the fabricated TENGs. The current load decreased, and the load voltage increased gradually with an increase in the external load resistance. The behavior is consistent with the internal impedance characteristics of the contact-separation TENGs. With a peak load voltage of ~8 V for PDMS/PEO-Al , the peak load current of PDMS/PEO-Cu was ~33 nA, and for PDMS/PEO-Al, the current was ~20 nA figure 11 shows combined graphs of load current and load voltage.

Power is calculated using the formula.

$$\boldsymbol{P = V^2/R} \quad (13)$$

Since the surface area is 2 cm^2, therefore.

$$\boldsymbol{Pd = \frac{P}{2}\ W/cm^2} \quad (14)$$

As illustrated above, power density can help find maximum load resistance. For this purpose, we took logarithm for power values, load resistance and applied polynomial equation on origin pro.

$$\boldsymbol{ax^2 + bx + c = 0} \quad (15)$$

After applying polynomial equation, power parameter displaced in resultant sheet have intercept value as c, B1 as ax^2 and B2 bx value. By applying differentiation on polynomial equations.

$$\boldsymbol{x = -\frac{b}{2a}} \quad (16)$$

As shown in figure 12 a characteristic parabolic curve was obtained. The PDMS/PEO-Al and PDMS/PEO-Cu combination gave the maximum peak power density of 10^{-8} W/cm², undoubtedly making it the most effective combination of electrodes during this stage of testing whereas other configurations like Al/PEO-Al and Cu/PEO-Al exhibited 10^{-10} W/m², and Cu/PEO-Cu gave lowest power density of about .

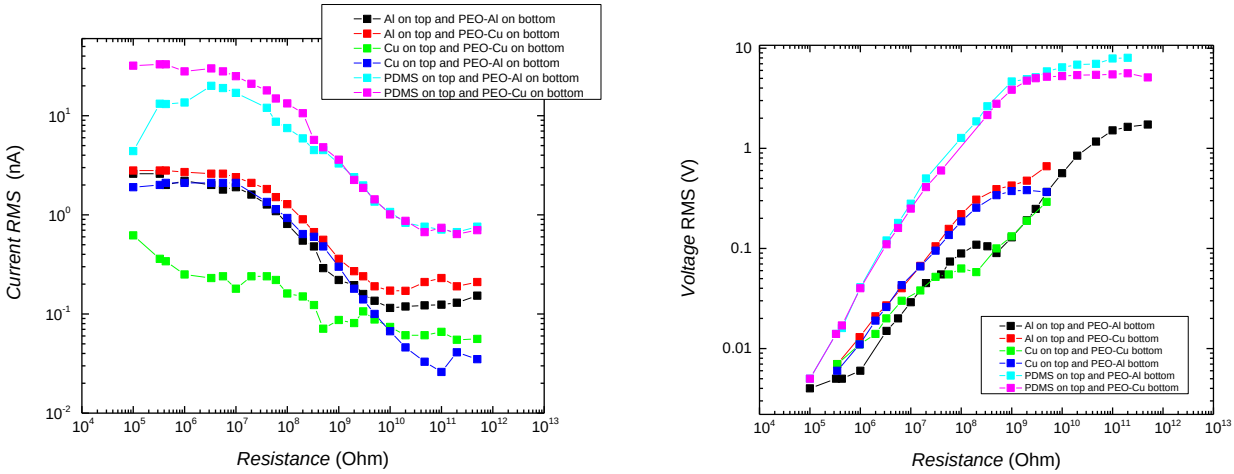

Figure 11: Combined graphs of Load current and Load voltage.

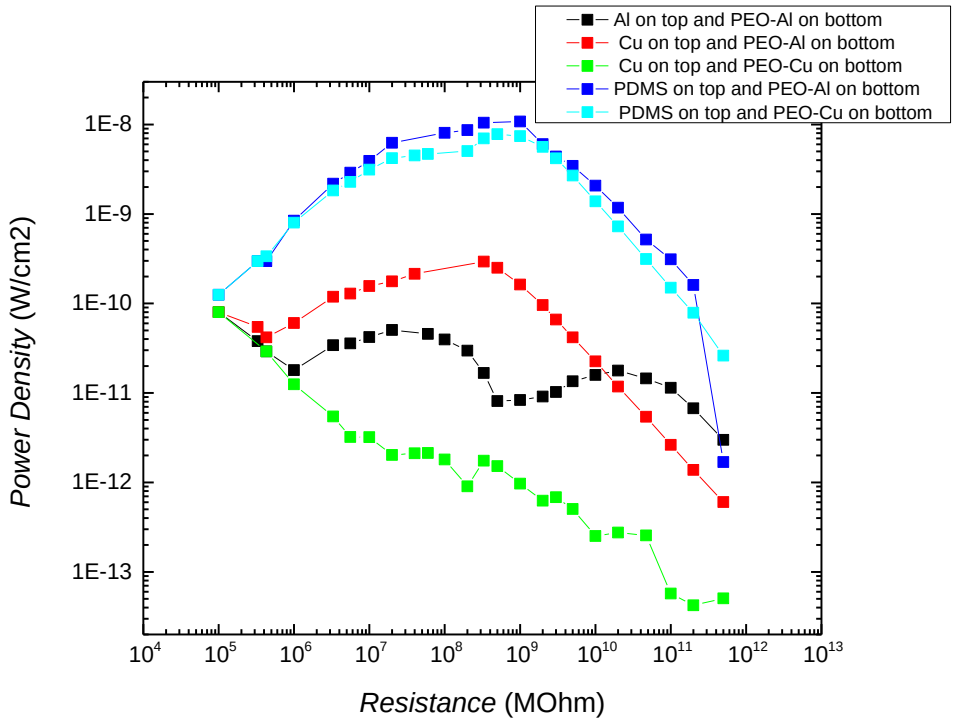

Figure 12: Power density graph

The steady increase in the trends of Voc, I_{SC}, surface charge density, and power density indicated that the triboelectric performance is not only affected by the conductivity of the electrode materials but also strongly depends on the polarity contrast between the contacting surface. Considering these results, the PDMS was chosen for further optimization studies with nanocomposites.

4.2 PEO with SiC, $BaTiO_3$, CNT's

In Phase 2, the contrast of dielectric polarity was shown to be important and use of high permittivity nanofillers in the PEO matrix was tried to improve its triboelectric performance. To investigate the charge

interaction mechanism, three different types of nanofillers were selected, namely multi-walled carbon nanotubes (CNT's), barium titanate ($BaTiO_3$) and silicon carbide (SiC).

The open circuit voltage results as shown in figure 13(b) indicated that the nanocomposites fabricated have a well-defined performance order. All the nanocomposite devices were made up of one active dielectric composite layer on the surface of the electrode, which meant that they were based on the single-dielectric model as depicted in figure 5(b). Therefore, (12) was used to investigate the effect of type and concentration of nanofiller on the change in the voltage output. The Voc values for the PEO/SiC composite and PEO/$BaTiO_3$ composite were ~76 V and ~60 V, respectively, higher than the values of the metal-only reference structures developed in case of pure PEO. The PEO/SiC composite exhibited a Voc of ~76 V and PEO/$BaTiO_3$ composite exhibited a Voc of ~60 V, which are higher than the metal-only reference structures developed in case of pure PEO.

The improvement in Voc is directly attributed to equation (12) which says that higher the surface charge density σ, higher is the voltage. The use of nanoparticles with a high permittivity allows an increase in charge accumulation at the interfaces after contact electrification, results to an increase in the polarization of the PEO matrix. The enhanced polarizability enhanced the effective charge trapping property of the dielectric layer and the layer's surface charge trapping amount.

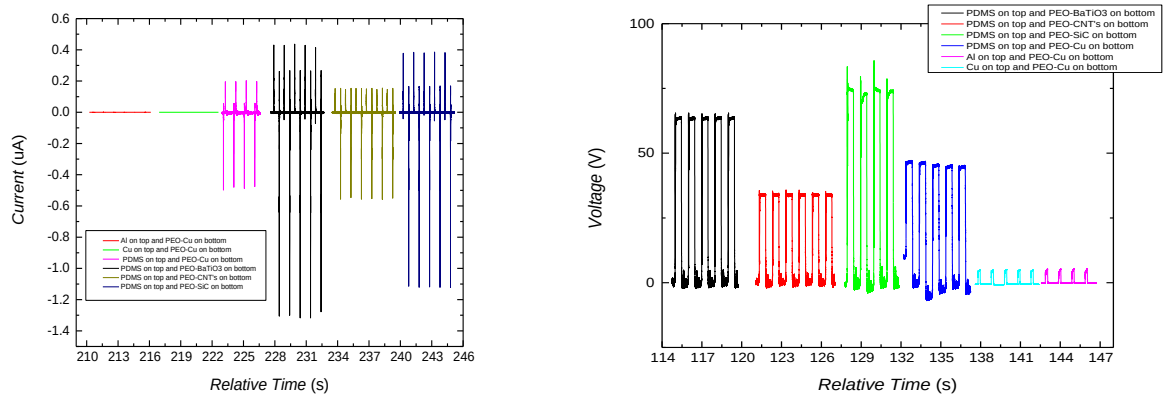

Figure 13:(a) Combined short circuit current graph. (b) Combined open circuit voltage graph

Although the permittivity of the PEO/SiC composite is not as high as that of $BaTiO_3$, the produced voltage was the maximum. This phenomenon shows that SiC has not only a polarization effect, but also a high number of surface trap states that can trap the triboelectric charge between cycles of voltage. The high effective σ and, hence, the large Voc is further reduced by the large bandgap of SiC, which also helps to reduce charge recombination.

The comparatively low voltage was explained as being due to the formation of conductive percolation pathways in the polymer matrix of the CNT composite. Some of the charges leaked through the conductive CNT network which lowered the effective charge-storage capacity and hence the surface charge density.

This was confirmed by the short-circuit current measurements. The amplitude of the PEO/SiC and

PEO/$BaTiO_3$ were large, being +0.4 to −1.3 μA and ±0.4 to −1.1 μA, respectively. The increased σ values that were obtained from the increased dielectric polarization as given in Equation (11) led to these larger currents. The currents in the PEO/CNT composite were relatively small because the conductive pathways neutralized part of the charges. figure 13(a) shows combined short circuit graphs of these samples.

The measurements of the surface charge density were more revealing of the role of the nanofillers. The equations utilized in finding charge density are illustrated below along with the table.

$$\sigma = \frac{Q}{A} \quad (17)$$

where Q is the total triboelectric charge, σ is the surface charge density, and A is the contact area. This equation highlights why increasing surface area through nano structuring and boosting charge density through material selection are critical for TENG performance.

$$Q = \int I_{SC}\, dt \quad (18)$$

$$\delta = \frac{1}{A}\int I_{SC}\, dt \quad (19)$$

As shown in figure 14. The surface charge density of the PEO/SiC composite was found to be highest with positive charge density of about +1.615 nC/cm², the PEO/$BaTiO_3$ composite had the highest negative surface charge density of nearly −1.683 nC/cm². Comparatively, the metal-only reference structures showed an interfacial-charge generation of around +0.093 nC/cm2, emphasizing the need for the use of dielectric nanofillers in enhancing the generation of charges at the interfaces.

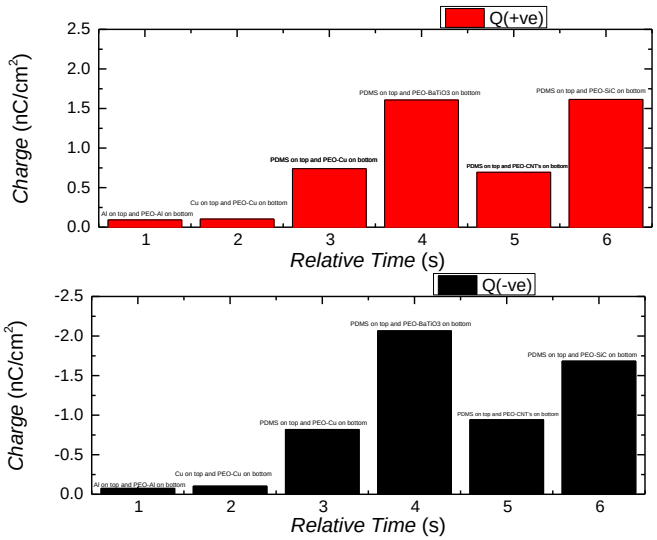

Figure 14: Surface charge transferred graph for both positive and negative cycles.

In terms of peak load voltage, the PEO/CNT composite was the best and achieved voltage of 13 V, slightly higher than that of PEO/$BaTiO_3$ and PEO/SiC composites, whose peak load voltage were about 12 V. The increased voltage production of the CNT composite under load conditions could be due to the increased

effective contact area and the localized electric field amplification which increases the apparent contact area's charge density under resistive loading. Not surprisingly, the metal-only systems (Al-PEO/Cu and Cu-PEO/Cu) retained their position as having the lowest load voltage values for all the resistances.

The load current behavior, as shown in figure 15, showed that PEO/SiC had the largest RMS load current of around 0.067 μA and PEO/$BaTiO_3$ had the RMS load current of 0.057 μA. The CNT composite had a relatively low load current, which is explained by the charge trapping effect, increased internal impedance, and partial polarization saturation of the conductive network of the composite. Overall, these results make PEO/SiC the most balanced and consistently high performing composite in all four electrical parameters tested.

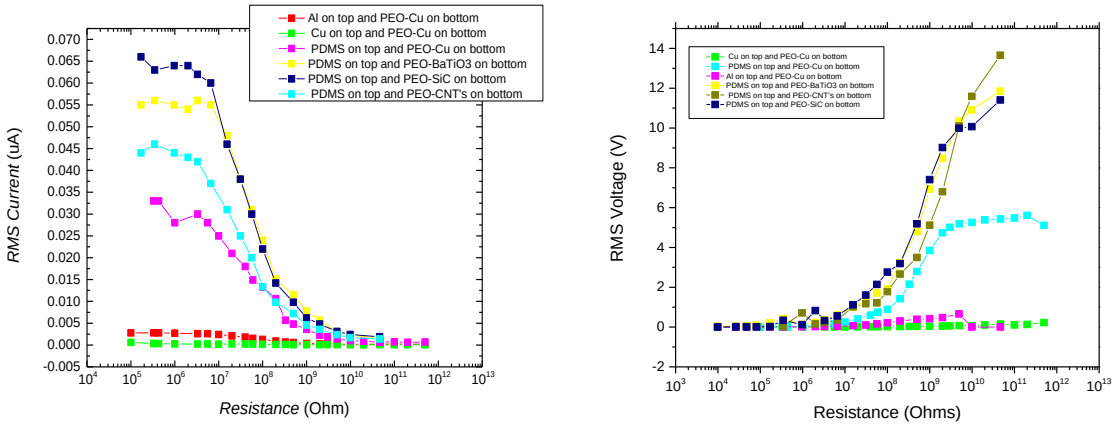

Figure 15:(a) Load current graphs under varying load condition. (b) Load voltage graphs under varying load conditions.

The composite PEO/SiC had the highest RMS load current (0.067μA) and the most uniform load dependent power generation and surface charge density in all the measured output parameters of the composites. So, the PEO/SiC composite was chosen for the optimization of concentration in Phase 3.

4.3 PEO With Different Sic Concentrations

In the final stage of the above work, the concentration of SiC nanoparticles in PEO matrix was systematically optimized and the amount of SiC nanoparticles that would provide the optimal energy harvesting performance of the triboelectric generator was determined. Seven different formulations containing SiC content of 0.025, 0.075, 0.1, 0.3, 0.5, 1, and 5 vol% were prepared and tested.

There was a clear non-monotonic response of electrical output to SiC concentration. All the measured parameters first increased as SiC loading increased, peaked at 0.1 vol%, and then gradually decreased as the loading was further increased.

When the concentration of SiC nanoparticles is low, the nanoparticles are well dispersed and will enhance the amount of dielectric polarization and avoid forming aggregates of nanoparticles that can act as charge trapping sites. This will result in a higher surface charge density σ, and a higher Voc and Isc as shown in Equations

(11) and (12).

These results in terms of the open-circuit voltage as shown in figure 16 clearly showed such concentration dependence. The voltage output of the composite became highest with value of -95V as it was more concentrated, reaching 0.1 vol%, and then decreased slowly as it became more concentrated still. The loss of effective charge trapping at high concentrations of SiC is consistent with more SiC contributing to the loss of effective charge trapping, so that the overall surface charge density decreases.

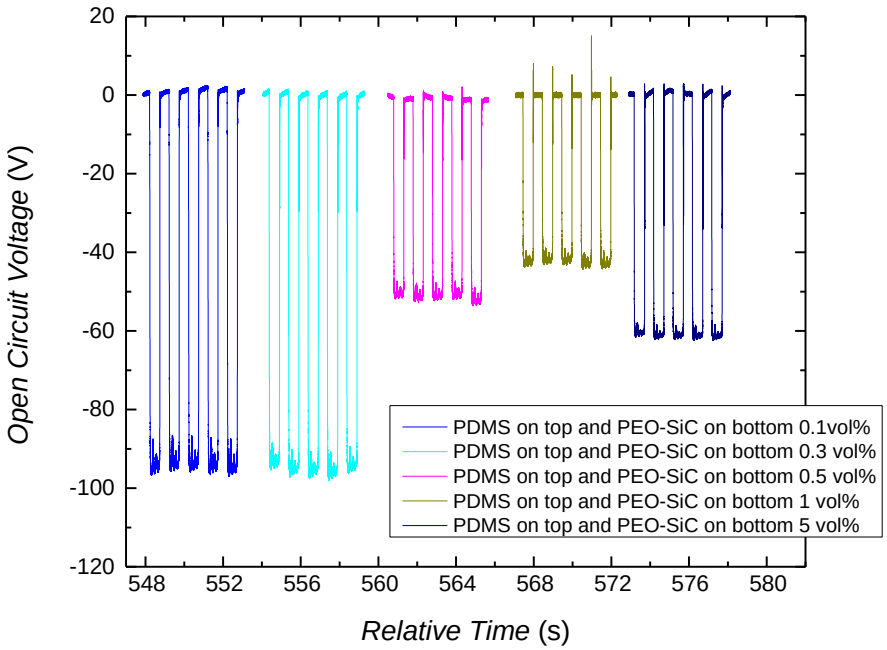

Figure 16: Open Circuit Voltage

The measurements of short circuit current that were also conducted showed even more evidence of an optimum concentration figure 17 shows short circuit current graphs for the tested samples. The concentration-dependent devices (PEO/SiC) gave a concentration-dependent current behavior as illustrated in the figure 5(b) configuration and the resulting current behavior was understood based on Equation (11), which is a direct function of the concentration of SiC, free layer thickness d0 and separation velocity. The 0.1 vol% sample yielded a peak-to-peak current of ~ ±2.3μA, which was over four times that of the 0.025 and 0.075 vol% samples, and almost five times that of the higher loading samples.

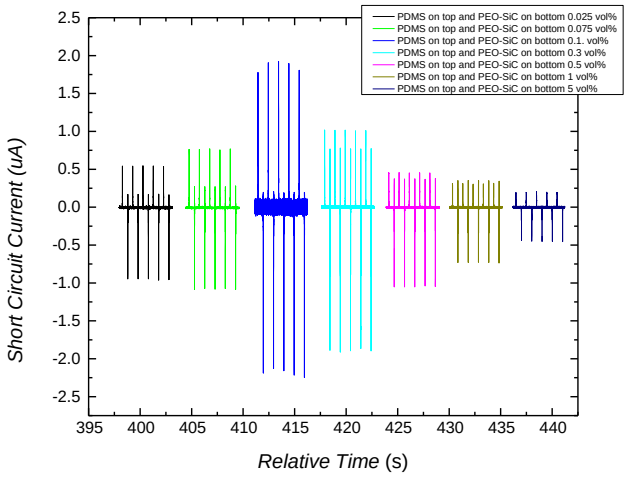

Figure 17: Short Circuit Current

This is a good strengthening which can be accounted for by equation (11). Both σ and effective dielectric parameter d_0 had positive values at 0.1 vol% which were good for maximizing charge transfer for the contact-separation cycle. This concentration, and beyond, resulted in charge storage capacity decreasing due to the presence of conduction pathways created by agglomeration, which led to a current output decrease.

The best behavior was quantified in the measurements of surface charge density. As shown in table 2 and figure 18 The density of positive and negative charges both increased continuously with increasing concentration of SiC up to the volume concentration of 0.1 vol% SiC and had the maximum concentrations of +2.59 nC/cm² and −2.33 nC/cm², respectively. These concentrations are about 100% higher than the lowest concentration sample.

Both the positive and negative surface charge density decreased in a systematic manner beyond the optimum concentration. The measured ones at 5 vol% SiC were +0.857 nC/cm² and −0.869 nC/cm², respectively. The degradation rate decreases monotonically, indicating that the main degradation pathway becomes the one of agglomeration of the nanoparticles at high filler concentrations.

Table 2: Surface Charge Density of Each Concentration

PDMS on top and PEO-SiC on bottom Vol%	**Q(+ve) nC/cm²**	**Q(-ve) nC/cm²**
0.025	1.29	-1.43
0.075	1.42	-1.41
0.1	2.59	-2.33
0.3	2.35	-2.1
0.5	1.56	-1.32

1	0.99	-0.89
5	0.857	-0.869

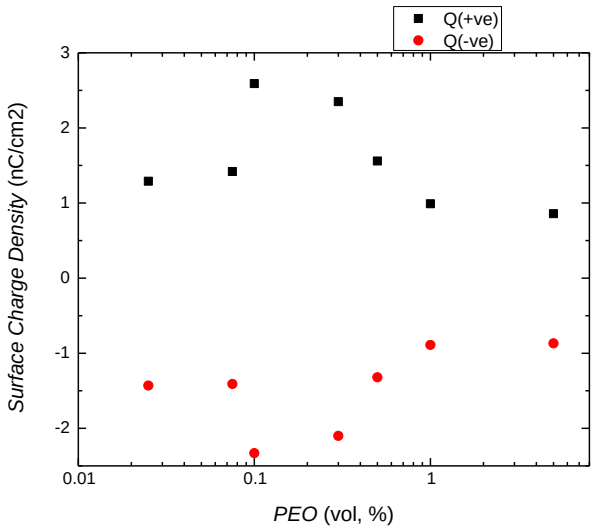

Figure 18: Surface Charge Density

The three samples with the best performance (0.075, 0.1 and 0.3 vol% SiC) were then tested under load-dependent electrical measurements. The load voltage of RMS device exhibited the typical impedance matching phenomenon of contact-separation TENGs their output can be observed in figure 19. When the external resistance was low, the voltage was small since the majority of charges that were produced passed through the external circuit. As resistance rose the voltage slowly got closer to saturation.

There was the steepest voltage rise in the sample containing 0.1 vol%. This voltage output was the greatest at the relatively low resistance levels in this sample, which were approximately 15V. This behavior suggests low internal impedance and good impedance matching behavior for real-world energy harvesting applications.

As expected, the measurements of RMS load currents decreased monotonously with the increase of load resistance as shown in figure 20. For the lowest resistance tested (10^4 Ω), the sample of 0.3 vol% of the current was the highest, around 0.065-0.070 µA, followed by the current of the sample of 0.1 vol% and the current of the sample of 0.075 vol%. Despite the slightly smaller sample size at low resistance, the 0.3 vol% sample internal resistance and charge retention was higher resulting in a decrease in total power generation capability.

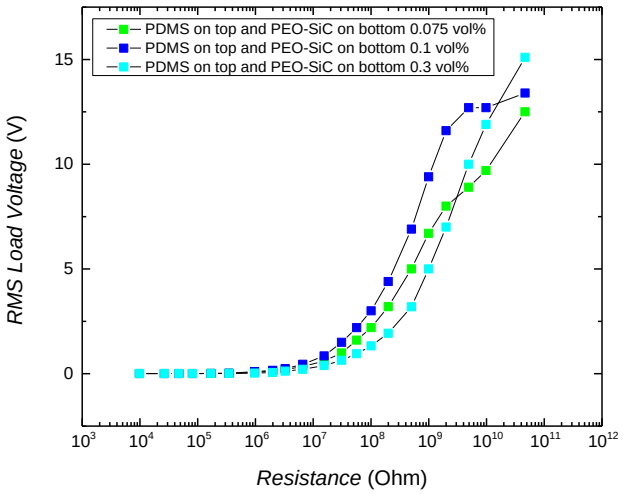

Figure 19: RMS Load Voltage

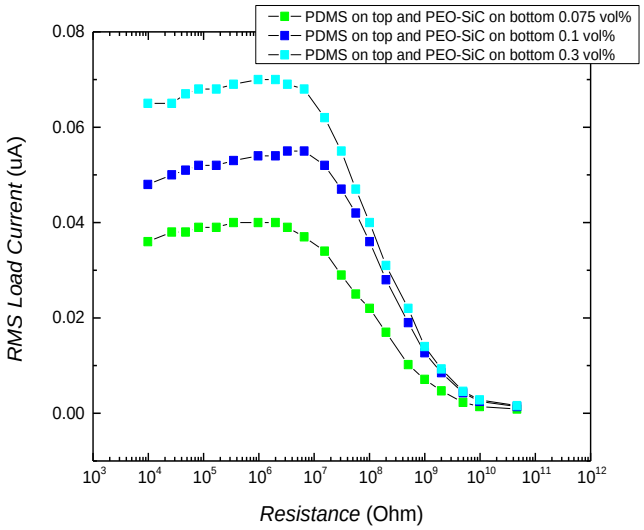

Figure 20: RMS Load Current

Power density analysis was the most direct measurement used to determine the most optimum concentration. All of the samples had the common power-density curve as a function of load resistance, with the maximum power obtained at the point where the external resistance value is equal to the internal resistance value of the TENG. For this purpose, we calculated power by using voltage measured over relative time at individual load. Later, this power is integrated and area under the power curve for every pulse was calculated. Formula for power and the values at optimal resistances are mentioned below in Table 3 and figure21.

$$A_0 = \int_{x_1}^{x_2} P_{inst}(t)\, dt \qquad (20)$$

$$P_{avg} = \frac{A_0}{x_2 - x_1} \qquad (21)$$

Where, P_{avg} represent the statics value taken for prepared sample. Later, we applied gaussian method, since the power density graph showed in figure 21 has bell shaped peaks. These bell-shaped peaks represent the area where power is maximum over the range of resistive load. Therefore, after applying gaussian method, optimal resistance and power density is further calculated by using these equations.

$$R^{max} = 10^{x_c} \quad (22)$$

$$P.d = y_0 + A \quad (23)$$

The composite with 0.1 vol% showed the highest maximum peak power density of 9.325×10^{-7} W/cm2 at optimum value of resistance of 10.62 MΩ. In comparison, the 0.075 vol% sample produced 5.717×10^{-7} W/cm² at 7.96 MΩ, while the 0.3 vol% sample generated only 2.842×10^{-7} W/cm² at a significantly higher resistance of 21.26 MΩ.

Table 3: Power Density of samples against load resistance

PDMS on top and PEO-SiC on bottom Vol%	**R^{max} MΩ**	**Pd W/cm²**
PEO 0.075 vol %	7.95884	5.7171E-7
PEO 0.1 vol %	10.62038	9.325E-7
PEO 0.3 vol %	21.25935	2.8419E-7

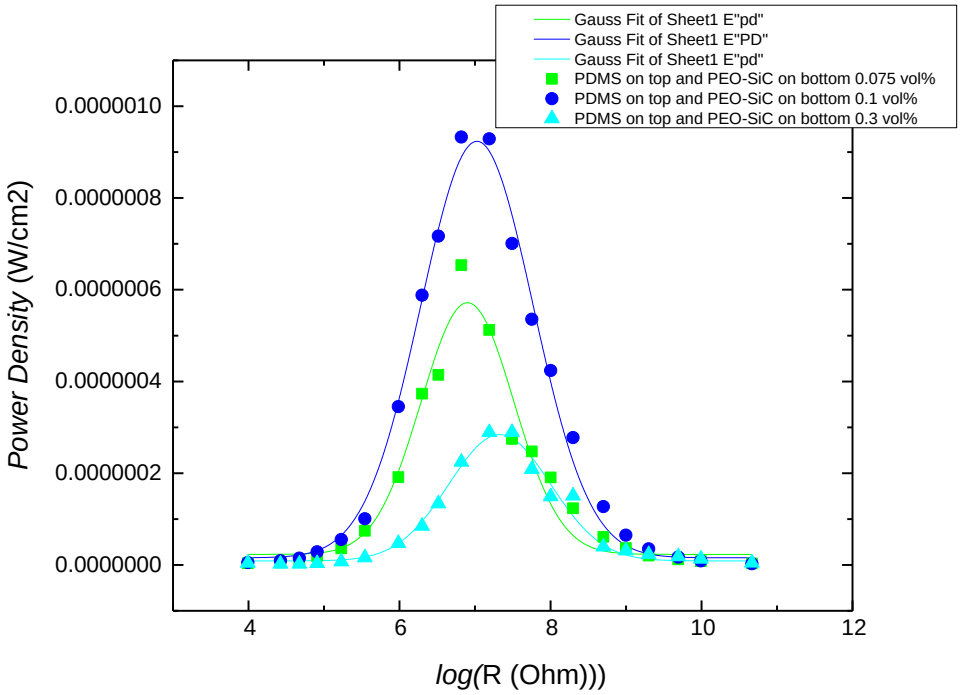

Figure 21: Power Density Graph

When the content of SiC increases, the optimal resistance increases, which specifies that the internal impedance increases as the SiC content increases, the internal dielectric coefficient decreases, and a certain degree of agglomeration of nanoparticles exists. The nanoparticles were well dispersed in the PEO matrix at the concentration of 0.1 vol% SiC, which lead to the maximum dielectric enhancement and charge trapping efficiency, impedance matching and surface charge density.

CONCLUSION

- After investigating different PEO/metal and PDMS/PEO TENG configuration, the best result was with PDMS counter layer, giving V_{OC} of 90 V, I_{SC} of 0.2μA, Load Current of ~33nA and power density of 10^{-8} W/cm².

- Adding fillers like $BaTiO_3$, SiC and CNT's we found that PEO/SiC gave the best values with V_{oc} of ~76 V, Isc of 0.4 μA, surface charge density of +1.615nC/cm^2.

- Seven different SiC concentrations ranging from 0.025-5%vol were tested and best results were obtained for 0.1 vol% SiC with V_{OC} of -95V, I_{SC} of 2.3 μA and, surface charge density of +2.59/−2.33 nC/cm² and highest power density of 9.325×10^{-7} W/cm² at optimum PEO resistance of 10.62 MΩ.

REFERENCES

1. S. M. Vahidhosseini, S. Rashidi, and M. H. Ehsani, "Enhancing sustainable energy harvesting with triboelectric nanogenerators (TENGs): Advanced materials and performance enhancement strategies," Renewable and Sustainable Energy Reviews, vol. 216, p. 115663, Jul. 2025, doi: https://doi.org/10.1016/j.rser.2025.115663.

2. Haroun, M. Tarek, M. Mosleh, and F. Ismail, "Recent Progress on Triboelectric Nanogenerators for Vibration Energy Harvesting and Vibration Sensing," Nanomaterials, vol. 12, no. 17, p. 2960, Aug. 2022, doi: https://doi.org/10.3390/nano12172960.

3. Z. L. Wang, "Triboelectric nanogenerators as new energy technology and self-powered sensors – Principles, problems and perspectives," Faraday Discuss., vol. 176, pp. 447–458, 2014, doi: https://doi.org/10.1039/c4fd00159a.

4. P. Ding et al., "Realizing the potential of polyethylene oxide as new positive tribo-material: Over 40 W/m2 high power flat surface triboelectric nanogenerators," Nano Energy, vol. 46, pp. 63–72, Jan. 2018, doi: https://doi.org/10.1016/j.nanoen.2018.01.034.

5. S. Feng et al., "Synergistic Effects of $BaTiO_3$/Multiwall Carbon Nanotube as Fillers on the Electrical Performance of Triboelectric Nanogenerator Based on Polydimethylsiloxane Composite Films," Energy technology, vol. 7, no. 6, Apr. 2019, doi: https://doi.org/10.1002/ente.201900101.

6. Zhao, K., Sun, W., Li, S. et al. Rational design on high-performance triboelectric nanogenerator consisting of silicon carbide@silicon dioxide nanowhiskers/polydimethylsiloxane (SiC@SiO_2/PDMS) nanocomposite films. Discover Nano **18**, 69 (2023). https://doi.org/10.1186/s11671-023-03822-8

7. V.-L. Trinh and C.-K. Chung, "Advances in Triboelectric Nanogenerators for Sustainable and Renewable Energy: Working Mechanism, Tribo-Surface Structure, Energy Storage-Collection System, and Applications," Processes, vol. 11, no. 9, p. 2796, Sep. 2023, doi: https://doi.org/10.3390/pr11092796.

8. H. Han, “Triboelectric Nanogenerators: From Basic Mechanisms to Sustainable Energy Applications,” Applied and Computational Engineering, vol. 181, no. 1, pp. 128–139, Sep. 2025, doi: https://doi.org/10.54254/2755-2721/2025.gl26560.

9. J. Shao, T. Jiang, and Z. Wang, “Theoretical foundations of triboelectric nanogenerators (TENG),” Science China Technological Sciences, vol. 63, no. 7, pp. 1087–1109, May 2020, doi: https://doi.org/10.1007/s11431-020-1604-9.

10. G.-J. Choi, S.-H. Sohn, S.-J. Kim, and I.-K. Park, “Polymer Composite-Based Triboelectric Nanogenerators: Recent Progress, Design Principles, and Future Perspectives,” Polymers, vol. 17, no. 14, p. 1962, Jul. 2025, doi: https://doi.org/10.3390/polym17141962.

11. S. Rathore, S. Sharma, B. P. Swain, and R. Kr. Ghadai, “A Critical Review on Triboelectric Nanogenerator,” IOP Conference Series: Materials Science and Engineering, vol. 377, p. 012186, Jun. 2018, doi: https://doi.org/10.1088/1757- 899x/377/1/012186.

12. J. Luo, W. Gao, and Z. L. Wang, “The Triboelectric Nanogenerator as an Innovative Technology toward Intelligent Sports,” Advanced Materials, vol. 33, no. 17, p. 2004178, Mar. 2021, doi: https://doi.org/10.1002/adma.202004178.

13. N. Kaur and K. Pal, “Triboelectric Nanogenerators for Mechanical Energy Harvesting,” Energy Technology, vol. 6, no. 6, pp. 958–997, May 2018, doi: https://doi.org/10.1002/ente.201700639.

14. X. Pu, S. An, Q. Tang, H. Guo, and C. Hu, “Wearable triboelectric sensors for biomedical monitoring and human-machine interface,” iScience, vol. 24, no. 1, p. 102027, Jan. 2021, doi: https://doi.org/10.1016/j.isci.2020.102027.

15. R. Walden, C. Kumar, D. M. Mulvihill, and S. C. Pillai, “Opportunities and Challenges in Triboelectric Nanogenerator (TENG) based Sustainable Energy Generation Technologies: A Mini-Review,” Chemical Engineering Journal Advances, vol. 9, p. 100237, Mar. 2022, doi: https://doi.org/10.1016/j.ceja.2021.100237.

16. D. W. Kim, J. H. Lee, J. K. Kim, and U. Jeong, “Material aspects of triboelectric energy generation and sensors,” NPG Asia Materials, vol. 12, no. 1, Jan. 2020, doi: https://doi.org/10.1038/s41427-019-0176-0.

17. S. Pan and Z. Zhang, “Fundamental theories and basic principles of triboelectric effect: A review,” Friction, vol. 7, no. 1, pp. 2–17, Aug. 2018, doi: https://doi.org/10.1007/s40544-018-0217-7.

18. S. Niu et al., “Theoretical study of contact-mode triboelectric nanogenerators as an effective power source,” Energy & Environmental Science, vol. 6, no. 12, p. 3576, 2013, doi: https://doi.org/10.1039/c3ee42571a.

19. I. Aazem et al., “Electrode materials for stretchable triboelectric nanogenerator in wearable electronics,” RSC Advances, vol. 12, no. 17, pp. 10545–10572, 2022, doi: https://doi.org/10.1039/d2ra01088g.13

20. A. Nasri, Zulhakim Za'Aba, Nuraliza Noorawzi, W. Nursheila, Ridwan Yahaya, and S. Bahri, “Evaluation of the Electrical Performance of Single-Electrode Mode Triboelectric Nanogenerators Based on Different Conductor Materials,” pp. 141–145, Nov. 2024, doi: https://doi.org/10.1109/ieacon61321.2024.10797327.

21. G. Pace, A. Ansaldo, M. Serri, S. Lauciello, and F. Bonaccorso, “Electrode selection rules for enhancing the performance of triboelectric nanogenerators and the role of few-layers graphene,” Nano Energy, vol. 76, p. 104989, Oct. 2020, doi: https://doi.org/10.1016/j.nanoen.2020.104989.

22. A. Okbaz, A. Karabiber, A. Yar, Z. Kınas, A. Sarılmaz, and F. Ozel, “High-performance triboelectric nanogenerator with optimized Al or Ti-embedded silicone tribomaterial,” Energy Conversion and Management, vol. 252, p. 115053, Jan. 2022, doi: https://doi.org/10.1016/j.enconman.2021.115053.

23. P. Cerchier, L. Pezzato, C. Gennari, E. Moschin, I. Moro, and M. Dabalà, “PEO coating containing copper: A promising anticorrosive and antifouling coating for seawater application of AA 7075,” Surface and Coatings Technology, vol. 393, p. 125774, Jul. 2020, doi: https://doi.org/10.1016/j.surfcoat.2020.125774.

24. D. Tantraviwat, M. Ngamyingyoud, W. Sripumkhai, P. Pattamang, G. Rujijanagul, and B. Inceesungvorn, “Tuning the Dielectric Constant and Surface Engineering of a BaTiO3/Porous PDMS Composite Film for Enhanced Triboelectric Nanogenerator Output Performance,” ACS Omega, vol. 6, no. 44, pp. 29765–29773, Oct. 2021, doi: https://doi.org/10.1021/acsomega.1c04222.

25. J. Wang et al., “High-Performance Triboelectric Nanogenerator Based on Carbon Nanotube-Functionalized Supramolecular Polyrotaxane Composites,” ACS Applied Polymer Materials, vol. 7, no. 3, pp. 1300–1306, Jan. 2025, doi: https://doi.org/10.1021/acsapm.4c02987.

26. K. Lee et al., “Boosting triboelectric performance of PDMS-based nanogenerators through dual-filler embedded triboelectric layers,” Journal of Alloys and Compounds, vol. 1010, p. 177114, Oct. 2024, doi: https://doi.org/10.1016/j.jallcom.2024.177114.

27. Chrysostomos Papamichail, O. Techlemtzi, G. Nikolakakou, and Emmanouil Glynos, “Cation Chemistry and Molecular Weight Effects on the Ion Conductivity in PEO-based Electrolytes,” ACS Macro Letters, vol.14, no. 2, pp. 225–230, Feb. 2025, doi: https://doi.org/10.1021/acsmacrolett.4c00802.

28. X. Liu et al., “Improvement in the output performance of polyethylene oxide-based triboelectric nanogenerators by introducing core–shell Ag@SiO_2 particles,” Journal of Materials Chemistry C, vol. 10, no. 1, pp. 265–273, Nov. 2021, doi: https://doi.org/10.1039/d1tc04831g.

29. “Optical and Chemical Investigations of PEO Thin Films Incorporated with Curcumin Nanoparticle: Effect of Film Thickness,” Biointerface Research in Applied Chemistry, vol. 13, no. 2, p. 143, Mar. 2022, doi: https://doi.org/10.33263/briac132.143.

SUMMARY

Didėjanti tvariosios energijos paklausa ir TENG, kaip perspektyvaus atsinaujinančios energijos šaltinio, atsiradimas paskatino mus toliau tirti PEO pagrindu pagamintus TENG ir kaip galime pasiekti maksimalią galią naudodami skirtingas TENG konfigūracijas arba įtraukdami aktyvius užpildus į PEO pagrindu pagamintus. Pirmiausia kaip aktyvų triboelektrinį sluoksnį panaudojome PEO pagrindu pagamintą dielektrinę plėvelę ir šešių skirtingų elektrodų konfigūracijų derinį (Al/PEO_Cu, PDMS/PEO_Al, PDMS/PEO_Cu, Cu/PEO_Al, Cu/PEO_Cu, Al/PEO_Al). Atlikus tyrimą pastebėta, kad PEO pagrindu pagaminti TENGS su PDMS/PEO konfigūracija parodė geriausius rezultatus, kai LOJ buvo 90 V, ISC 0,2 µA, apkrovos srovė ~33 nA ir galios tankis 10-8 W/m². Nustatę, kad TENG veikimas labai priklauso nuo paviršių poliškumo kontrasto, toliau tyrėme krūvio sąveikos mechanizmą, naudodami trijų skirtingų tipų nano užpildus (CNT, BaTiO3, silicio karbidą (SiC)), ir pridėjome šiuos užpildus į PEO pagrindu pagamintus TENG, ištyrėme ir palyginome jų rezultatus ir pastebėjome, kad PEO/SiC pasižymi geriausiomis savybėmis tarp visų išbandytų užpildų, kai Voc yra ~76 V, Isc +0.4, -1.3 µA, paviršiaus krūvio tankis +1,615 nC/cm2, Irms 0,067 µA. Po to optimizavome SiC koncentraciją PEO matricoje ir nustatėme SiC dalelių koncentracijos kiekį, kuris užtikrintų optimalų energijos surinkimo našumą. Buvo paruoštos ir išbandytos septynios skirtingos koncentracijos, kurių SiC kiekis yra 0,025, 0,075, 0,1, 0,3, 0,5, 1 ir 5 tūrio %, o geriausi rezultatai gauti naudojant 0,1 tūrio % SiC, kurio paviršiaus krūvio tankis yra +2,59/-2,33 nC/cm², o didžiausia galia. Tankis – 9,325 × 10^{-7} W/cm², o optimali PEO varža – 10,62 MΩ. Rezultatai gerėja didėjant koncentracijai, tačiau kai koncentracija viršija tam tikrą ribą, krūvio perdavimo ir gaudymo efektyvumas pradeda mažėti, o tai sumažina TENG našumą esant didesnei koncentracijai. Gerai disperguotos nanodalelės, kurių SiC koncentracija yra 0,1 tūrio %, užtikrina maksimalų dielektrinį sustiprėjimą ir krūvio gaudymo efektyvumą, todėl gaunamas geriausias išvesties našumas.

Increasing demand of sustainable energy and emergence of TENGS as promising renewable energy source motivated us to further investigate PEO-based TENGS and how we can achieve maximum power output using different TENG configuration or incorporating active fillers into PEO based. We first used PEO- based dielectric film as active triboelectric layer and combination of six different electrode configurations(Al/PEO_Cu, PDMS/PEO_Al, PDMS/PEO_Cu, Cu/PEO_Al, Cu/PEO_Cu, Al/PEO_Al) were used and after investigation it was observed that PEO-based TENGS with PDMS/PEO configuration exhibited best results with V_{OC} of 90 V, I_{SC} of 0.2µA, Load Current of ~33nA and power density of 10^{-8} W/m². after discovering that performance of TENG highly depends on polarity contrast between the surfaces we further investigated charge interaction mechanism using three different types of nano fillers (CNTs ,$BaTiO_3$, silicone carbide (SiC) and added these fillers in PEO based TENGs and investigated and compared their results and observed that PEO/SiC shows best behavior among all the tested fillers with V_{oc} of ~76 V, Isc of +0.4,-1.3µA, surface charge density of +1.615nC/cm^2, Irms of 0.067 µA. After that, we optimized SiC concentration in PEO matrix and determined the amount of SiC particle concentration that would give optimal energy harvesting performance, Seven different concentrations containing SiC content of 0.025, 0.075, 0.1, 0.3, 0.5, 1, and 5 vol% were prepared and tested and best results were obtained for 0.1 vol% SiC with surface charge density of +2.59/−2.33 nC/cm² and highest power density of 9.325×10^{-7} W/cm² at optimum PEO resistance of 10.62 MΩ. Results improve with increase in concentration ,but when the concentration exceeds a certain limit charge transfer and charge trapping efficiency starts to decrease which decreases performance of TENGs at higher concentration. Well dispersed nanoparticles at the concentration of 0.1 vol% SiC, lead to the maximum dielectric enhancement and charge trapping efficiency resulting in best output performance.